Penerbit Akademia Baru

Journal of Advanced Research in Fluid Mechanics and Thermal Sciences

Journal homepage: www.akademiabaru.com/arfmts.html
ISSN: 2289-7879

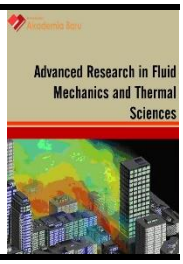

Evaluation of Hydro-Thermal Shell-Side Performance in a Shell-and-Tube Heat Exchanger: CFD Approach

Open Access

Suliman Alfarawi [1,*]

[1] Department of Mechanical Engineering, Faculty of Engineering, University of Benghazi, Libya

ARTICLE INFO

Article history:
Received 9 October 2019
Received in revised form 16 November 2019
Accepted 23 November 2019
Available online 26 February 2020

ABSTRACT

This work aims to improve a conventional shell-and-tube heat exchanger performance using three-dimensional computational fluid dynamics analysis based on finite element method (COMSOL Multiphysics software). Standard RANS k-ε turbulence model coupled with conjugate heat transfer model was adopted in the analysis. The influence of single-segmental baffles cut (25 %, 35 % and 45 %) and baffles number (4, 6 and 8) on hydro-thermal shell-side performance were investigated at nozzle-based Reynolds number varied from 5,500 to 12,000. The results showed that heat transfer and pressure drop increased by increasing the number of baffles and reducing baffles cut. However, the best thermal enhancement factor of 2.15, which is based on equal pumping power constraint, was obtained for the configuration of 35 % baffles cut and six baffles. To fill the gap in the literature, this study explores the importance of CFD in modelling shell-and-tube heat exchangers.

Keywords:
CFD Approach; Shell-and-tube; Heat Exchanger; Performance

1. Introduction

The proper utilization of energy resources can lead to the successful development of an efficient and cost-effective heat exchanger. A heat exchanger is a device that transfers thermal energy between a solid object and a fluid or between two or more fluids at different temperatures. Different heat exchangers are mainly distinct from each other according to flow direction; parallel-, counter- or cross-flow. Heat exchangers are abundant in various applications such as production lines and processing industries. An optimized design of the exchanger or improving the working fluid thermal properties using nanotechnology is being sought for efficient-conversion of heat transfer [1]. Shell-and-tube heat exchanger (STHX) is one of the most widely used types of heat exchangers in the processing industries [2]. The shell encloses a bundle of tubes with one fluid flows through the tubes and the other flows inside the shell. Normally, baffles are provided inside the shell to partly support the tube bundles and partly to intense turbulence of fluid flow for better heat transfer. Plate baffles are commonly used including; segmental, helical, orifice or disk-and-doughnut. Different

* *Corresponding author.*
E-mail address: s_s_s_elfarawi@yahoo.com (Suliman Alfarawi)

configurations of STHX were investigated by many researchers in terms of heat transfer and pressure drop characteristics using empirical or numerical methods.

The accurate determination of heat transfer coefficient in conventional and complex geometry heat exchangers is demanding for the initial design phase. Evaluation of shell-side performance of the heat exchanger has gained much attention in research by investigating several parameters to design an efficient heat exchanger. In literature, Bell-Delaware approach and Kern's method were widely used by many authors to analyze numerically heat exchanger performance or validate their models against these methods or experiments. However, the accuracy of both approaches is prone to the geometrical parameters' limitation of both methods [3]. Due to the shortage of basic information regarding the flow patterns associated with complex geometrical baffles, computational fluid dynamics approach (CFD) recently becomes a valuable tool in STHXs design and optimization. Bhutta *et al*., [4] intensively reviewed the use of CFD in the analysis of various heat exchangers proving its durability and accuracy. Nemati and Moghimi [5] explored CFD in simulating the complexity of fluid flow behavior inside an annular-finned tube heat exchanger using different turbulence models. Since the tube-side fluid flow and heat transfer characteristics of STHX is well-defined, most of the research is focused on shell-side performance enhancement.

A good technique to improve the shell-side performance of STHX is the optimization of baffles parameters including; baffles types, spacing, and cut. Using CFD to analyze the performance of STHX is not a simple task depending on the complexity of the geometry under investigation. Turbulence and conjugate heat transfer modelling using CFD sound accurate compared to other available numerical techniques, but excessive computational time and effort are demanding. There has been little research in open literature conducted on the use of CFD to simulate and enhance the performance of the standard STHXs compared to other numerical techniques and experiments. This highlights the possible outcomes of the current study based on the previous CFD studies performed on STHXs reviewed below.

Ozden *et al.,* [6] investigated numerically the effect of baffle spacing and baffle cut on the shell-side performance of single-segmental shell-and-tube heat exchanger using CFD analysis. The results showed that over increasing the baffles number from 6 to 12 and varying the baffle cut values from 36% to 25%, both heat transfer coefficients and pressure drop increased at different shell-side mass flow rates. Wen *et al.,* [7] studied numerically and experimentally the improvement of helical baffled STHX with a proposed ladder-type fold baffle. The numerical results obtained from ICEM CFD analysis demonstrated uniformity of fluid flow and elimination of dead zones in the proposed STHX. On the other hand, the thermal performance factor (TPF) is enhanced by 18.6–23.2%. Ambekar *et al.,* [8] studied the effects of different configurations of baffles on heat transfer coefficient and pressure drop in STHX. Single-, double-, triple segmental baffles, helical baffles, and flower baffles were investigated using CFD SOLIDWORKS Flow Simulations. It was shown that the overall heat transfer coefficient is descending from maximum with single segmental baffles, double segmental baffles, flower baffles, triple segmental baffles, to a minimum with helical baffles. However, flower baffles are the most effective baffles in terms of overall thermal performance (heat transfer to pressure drop).

El Maakoul *et al.,* [9] conducted a numerical study validated with an experiment on STHX with three types of baffles; trefoil-hole, helical baffles and the conventional segmental baffles. CFD simulations with ANSYS FLUENT were performed to evaluate the hydro-thermal characteristics of the three configurations. The results showed that the highest thermal performance index (heat transfer to pressure drop) was achieved at a lower mass flow rate for the case of helical baffles and worst-case with trefoil-hole. Bayram and Gökhan [10] studied the effect of variable baffle spacing on the thermal performance of shell-and-tube heat exchanger using CDF approach. Five spacing schemes

were considered in the investigation; one with equal baffle spacing, the second with centered baffle spacing, the third with sided baffle spacing, the fourth with inlet baffle spacing and the last with outlet baffle spacing. It was found that the first scheme had the lowest pressure drop and the highest heat transfer coefficient among all investigated cases.

Lei *et al.,* [11] adopted a CFD analysis to investigate the thermo-hydraulic performance of two novel shell-and-tube heat exchangers with louver baffles compared with conventional segmental baffles. Compared with the conventional at the same flow rate, the pressure drops were decreased by about 55% to 63% on average. It was found that the heat transfer coefficients per pressure drop of the two exchangers are about 73.3 to 118.2% higher than that of the STHX. Mellal *et al.,* [12] conducted CFD study using Comsol Multiphysics on a shell and tube heat exchanger under different baffle arrangements and orientation to evaluate hydro-thermal shell-side performance. Baffles spacing was varied from 106.6, 80, and 64 mm with six baffles orientation angles of 45, 60, 90, 120, 150, and 180, for Reynolds number ranging from 3,000 to 10,000. It was found that due to the zigzag flow mode with a short bypass with 10 baffles inclined by 180, the highest thermal performance factor of 3.55 at Re = 3,000 was realized. Wang *et al.,* [13] proposed a staggered arrangement of baffled STHX to replace segmental and helical baffles. CFD analysis using ANSYS FLUENT was carried out to study their fluid flow and heat transfer characteristics. Various parameters were investigated including baffle cut, stagger angle and baffle number, which optimally found to be from their results; 45%, 79° and 11, respectively.

Sadikin *et al.,* [14] studied numerically using a CFD approach, the influence of baffle numbers variation on shell-and-tube heat exchanger performance. Three cases were considered as the baffle numbers varied from 6 to 10 at a fixed mass flow rate of 5 kg/s. It was shown that increasing baffle numbers generates fewer recirculation zones in the shell-side of the exchanger suggesting that the 10-baffle case has the best thermal characteristics but with excessive flow resistance. Amini *et al.,* [15] performed a CFD study to investigate the effect of tube fins on the performance of shell-and-tube heat exchanger with a fixed number of baffles. Three configurations were adopted in the study; plain tubes, vertically finned tubes and helical fin tubes. The results showed that the exchanger effectiveness increased by 9.5% and 6% when using helical and segmented fins, respectively compared to plain tubes. Also, increasing fin height was found more effective than increasing the pitch for helical fin tubes. Ali and Reza [16] presented a CFD analysis of three baffle types (two disk-baffle and segmental baffles) combined with finned tube-bundles with different longitudinal ribbed shapes (without, circular and triangular ribs). The results showed that the disk baffled STHX with triangular ribbed tubes had the highest thermo-hydraulic performance.

This study aims to enhance the conventional STHX (horizontally single-segmented) performance using a 3D CFD model based on finite element method (COMSOL Multiphysics 5.3 software). The effect of single-segmental baffles cut and spacing on the hydro-thermal shell-side performance of STHX is investigated. The results of shell-side heat transfer coefficients and pressure drops for segmental baffles are validated with other available numerical methods. The best configuration in terms of optimum heat transfer to pressure drop is then recognized.

2. Model Description

The STHX under investigation [17,18] is comprised of 37 tubes having a (60°) triangular pitch arrangement and 500 mm length with horizontal single segmental baffles had a varied baffle cut in the range of (25, 35 and 45%) and varied baffles spacing in the range of (100, 60 and 42.85 mm) according to baffles numbers (4, 6, 8 baffles). STHX with 25% baffle cut and 4 baffles is drawn within

Comsol geometry builder and schematically shown in Figure 1. Table 1 summarizes all geometrical and operational parameters of STHX.

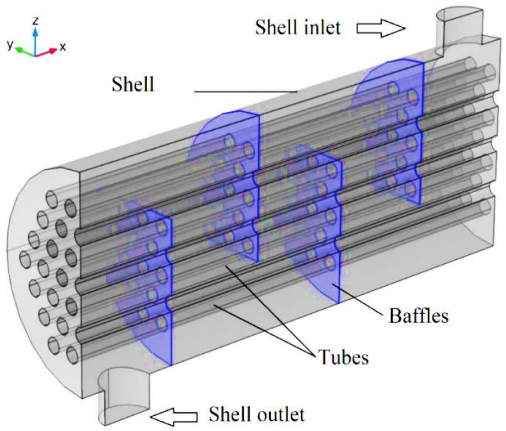

Fig. 1. STHX arrangement with 4 baffles and 25% baffle cut

Table 1
Geometrical and operational parameters of STHX [17,18]

Designation	Value/Unit
Baffle cut (B_c)	25, 35, 45%
Heat exchanger length (L)	500 mm
Shell nozzle diameter	50 mm
Number of Baffles (N_B)	4, 6, 8
Number of tubes (N_t)	37
Longitudinal pitch (P_t)	25 mm
Shell inside diameter (D_S)	200 mm
Tube outer diameter (d_o)	15 mm
Working fluid	Water
Inlet water temperature	298.15 K

2.1 Boundary Conditions

Symmetry boundary condition can afford a faster solution in which half of the STHX is chosen as a computational domain as depicted in Figure 1. A constant wall temperature of 353.15 K is imposed on their external tube walls to avoid modulating heat transfer and fluid flow through the tube-side. The baffles' walls are treated as internal walls. A thin aluminium layer of 2 mm is applied to shell structures and tubes to account for net heat flux to the shell-side. All the walls are treated as wall function including the shell, tubes and baffles [17]. The inlet shell side velocity of the fluid is varied based on nozzle's Reynolds numbers in the range between 5,500 to 12,000 with 1500 increment. Moreover, the outlet shell side is exposed to atmospheric pressure with normal flow condition.

2.2 Mesh Selection and Solver Settings

Within COMSOL Multiphysics environment, unstructured mesh with a varying element size for higher aspect ratios is well suited for the geometry of the investigated STHX. The algorithm by default uses free tetrahedral element and boundary layers to mesh the computational domain with dense mesh around the tubes and the baffles as shown in Figure 2.

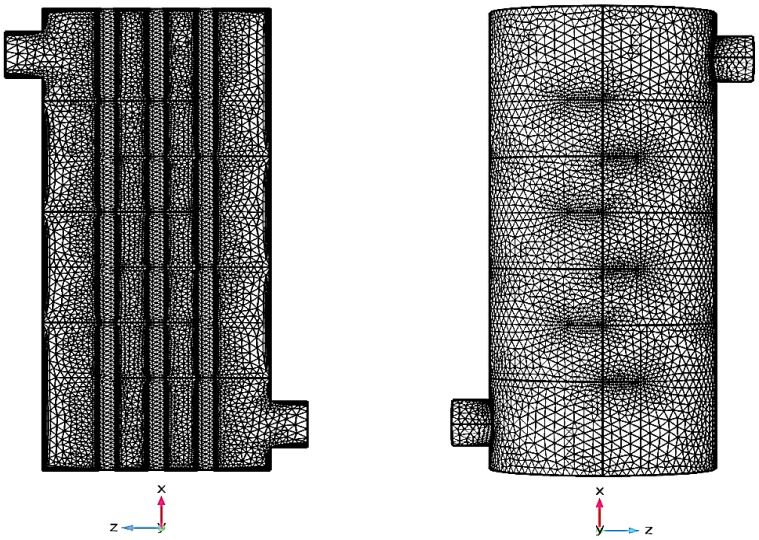

Fig. 2. Meshed geometry with tetrahedral element type

Based on the finite element method, the discretized governing equations of fluid flow and heat transfer (continuity, momentum, and energy equations) are solved by segregated solvers using iterative methods that require less memory compared to the direct solver in a fully coupled model. The algebraic multi-grid (AMG) solver with Parallel Sparse Direct Linear Solver (PARDISO) as a pre-conditioner provide robust solutions for large CFD simulations [17]. All simulations were performed on Intel(R) core (TM) CPU i7-4820K PC runs at a speed of 3.7 GHz with 48 GB RAM memory. To judge the accuracy of the current CFD results, testing metrics of CFD simulations are performed through mesh sensitivity analysis. Mesh sensitivity analysis was initially performed with different element sizes at minimum and maximum mass flow rates for the case of 25% baffle cut and 4 baffles as shown in Table 2. The total number of elements varies considerably from 289,531 to 1,444,963 for only half of the shell-side of the STHX. Grid-3 was selected to carry out simulations as the variation of the heat transfer coefficient and pressure drop values did not exceed 1.75% of that obtained when increasing the grid density to Grid-4 size.

Table 2
Mesh sequence and its sensitivity

Mesh size	Number of elements	$\dot{m} = 0.1066$ kg/s		$\dot{m} = 0.232$ kg/s	
		h (W.m^2/K)	Δp (Pa)	h (W.m^2/K)	Δp (Pa)
Grid-1	289,531	550.4	31.146	932.64	136.42
Grid-2	608,940	603.47	30.509	1040.8	134.18
Grid-3	795,687	623.48	29.813	1081.8	133.7
Grid-4	1,444,963	630.4	29.29	1100.7	131.36

2.3 Mathematical Formulation

The conjugate heat transfer model is adopted in this study based on Reynolds-Average Navier-Stokes (RANS) standard k-ε turbulence model. Using a non-isothermal flow assumption allows the computation of fluid flow properties according to temperature change. The resulting governing equations for stationary incompressible non-isothermal flow model (Mach number < 0.3) are

Continuity equation

$$\nabla.(\rho u) = 0 \tag{1}$$

Momentum equation

$$\rho(\nabla.u)u = -\nabla p + \nabla.(\mu + \mu_T)(\nabla u + (\nabla u)^T) \tag{2}$$

Energy equation

$$\rho C_p u(\nabla T) = \nabla.(K\nabla T) \tag{3}$$

The additional equations for k-ε standard turbulence model are based on the turbulent kinetic energy k, Eq. (4) and the energy dissipation ε, Eq. (5)

$$\rho(u.\nabla)\mathrm{k} = \nabla.\left[\left(\mu + \frac{\mu_T}{\sigma_k}\right)\nabla\mathrm{k}\right] + P_k - \rho\varepsilon \tag{4}$$

$$\rho(u.\nabla)\varepsilon = \nabla.\left[\left(\mu + \frac{\mu_T}{\sigma_\epsilon}\right)\nabla\epsilon\right] + C_{\varepsilon 1}\frac{\varepsilon}{\mathrm{k}}P_k - C_{\varepsilon 2}\rho\frac{\varepsilon^2}{\mathrm{k}} \tag{5}$$

where the production term P_k is defined as

$$P_k = \mu_T[\nabla u:(\nabla u + (\nabla u)^T)] \tag{6}$$

The turbulent viscosity is modelled as

$$\mu_T = \rho C_\mu \frac{\mathrm{k}^2}{\varepsilon} \tag{7}$$

The following values of empirical constants are assigned for as

$C_{\varepsilon 1}$ =1.44, $C_{\varepsilon 2}$ = 1.92, C_μ= 0.09, σ_k = 1, σ_ϵ = 1.3

The heat transfer coefficient, h is calculated from the knowledge of net heat flux transferred from tubes bundle to the shell side, q'', the average wall temperature, T_w and the fluid bulk temperature in the shell side, T_b.

$$h = q''_{net}/(T_w - T_b) \tag{8}$$

The friction factor can be calculated based on the pressure drop (Δp) that obtained from simulations. Since the outlet of the nozzle exposed to atmospheric pressure (zero-gauge pressure), the pressure drop is practically the pressure at the inlet nozzle,

$$f = \frac{2}{(L/D_h)}\left(\frac{\Delta p}{\rho u^2}\right) \tag{9}$$

The thermal performance factor η based on the constraint of equal pumping power is defined by

$$\eta = (Nu/Nu_0)/(f/f_0)^{\frac{1}{3}} \quad (10)$$

where Nu_0 & f_0 are respectively, the Nusselt number and the friction factor for the reference case (STHX without baffles).

3. Results and Discussion

3.1 Results Validation

Kern's method [19] and the log mean temperature method (LMTD) [20] are adopted to validate the CFD model results of heat transfer coefficient and pressure drop results. Kern's method is an experimentally-based approach for standard STHX configuration, and it is simple to apply. The LMTD method is used to calculate the convective heat transfer coefficient of the shell-side with the knowledge of net heat transferred from tube bundles to the shell-side. The procedure steps of both methods are illustrated and summarised in Table 3.

Table 3
Summary of Kern's method and LMTD method procedures [19,20]

Kern's method procedure	
Parameter	Equation
Equivalent diameter (mm)	$D_e = 4[P_t^2 - (0.25\pi d_o^2)]/\pi d_0$
Shell-side mass velocity (kg/m^2)	$G_s = \dot{m}/A_s$
Cross-flow area (m^2)	$A_s = (P_t - d_0).D_s.B_s/P_t$
Shell-side Reynolds number	$Re_s = G_s.D_e/\mu$
Shell-side velocity (m/s)	$u_s = G_s/\rho$
Shell-side heat transfer coefficient (W.m^2/K)	$h = j_h.\left(\frac{k}{D_e}\right).Re_s.Pr^{0.33}(\frac{\mu}{\mu_w})^{0.14}$
Shell-side pressure drop (Pa)	$\Delta p = 8j_f.\left(\frac{D_s}{D_e}\right).\left(\frac{L}{B_s}\right).\frac{\rho u_s^2}{2}.\left(\frac{\mu}{\mu_w}\right)^{-0.14}$
LMTD method procedure	
Heat transfer rate to the shell side (W)	$\dot{Q} = \dot{m}C_p(T_{out} - T_{in})$
Temperature differences (K)	$\Delta T_{max} = T_w - T_{in}, \Delta T_{min} = T_w - T_{out}$
LMTD	$\Delta T_{max} - \Delta T_{min}/\ln(\Delta T_{max}/\Delta T_{min})$
Heat transfer area (m^2)	$A_o = N_t.\pi.d_0.L$
Shell-side heat transfer coefficient (W.m^2/K)	$h = \dot{Q}/LMTD.A_o$

where the factor (j_f) and (j_h) are obtained from the charts for segmental baffles [3].

It is not feasible to compare all CFD results with the above-mentioned methods. However, the number of baffles is fixed to 8 and baffle cut is varied within the specified range to perform a comparison. Figure 3 presents the comparison of CFD results against Kern's method and LMTD method for heat transfer coefficients and the pressure drops versus shell-side mass flow rates at fixed baffle number (8) and various baffle cut (25%, 35%, and 45%).

Fairly good agreement was found between simulation results and Kern's method. A maximum deviation of 23% is noted between the present study and Kern's method for pressure drop in the case of 45% baffles cut at a maximum mass flow rate (Figure 3(f)). For heat transfer coefficient results, the maximum deviation is 17.4% in the case of 35% baffles cut at a maximum mass flow rate (Figure 3(c)). In general, Kern's method underestimates shell-side pressure drop due to the assumption of idealized main-stream flow (the actual stream is cross-flow between baffles and axial (parallel) flow through baffles windows). On the other hand, the present results of convective heat transfer

coefficients compare very well with the LMTD method where the maximum deviation did not exceed 9% as depicted in Figure 3(a) with a 25% baffle cut at the lowest mass flow rate. This proves the reliability of the current CFD model and the accuracy of its simulation results.

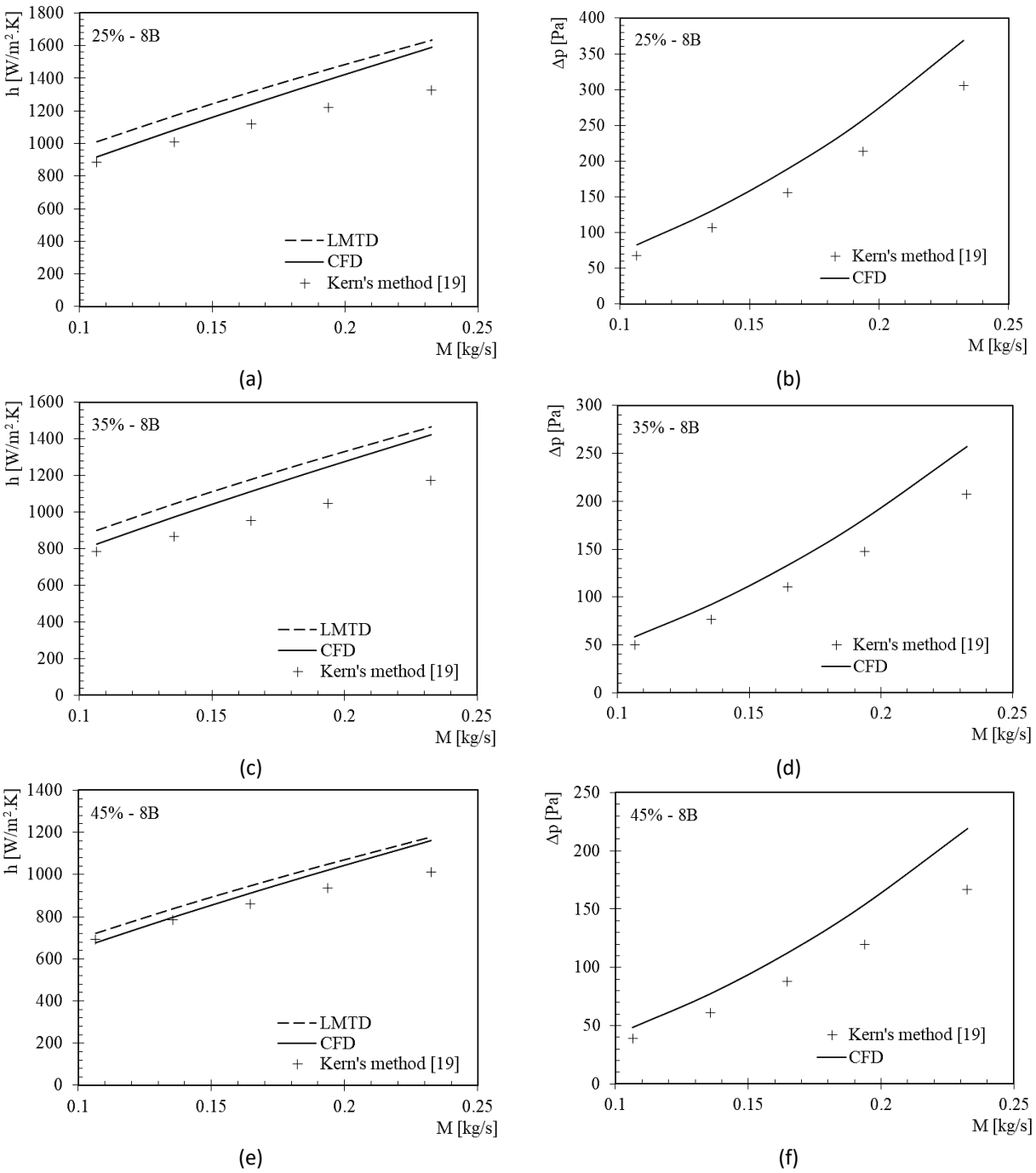

Fig. 3. Comparison of CFD results of heat transfer coefficients and pressure drops at various baffle cuts and fixed number of baffles (8) with available numerical methods

3.2 Fluid Flow

The flow behaviour in the shell-side of STHX at 35% baffle cut and various baffle spacings at maximum mass flow rate is visualized in Figure 4. The zigzag flow pattern is clearly observed for all baffle spacings characterized by cross-flow streams. The fluid flow is attached to the walls of baffles

and tubes as the viscous boundary layer starts to develop due to the no-slip condition. As the fluid flows past the tubes, momentum change at each segmental baffle causes a separation in the main flow at the rear of the baffle and re-attachment of the flow at the front of the baffle where recirculation and dead zones are generated.

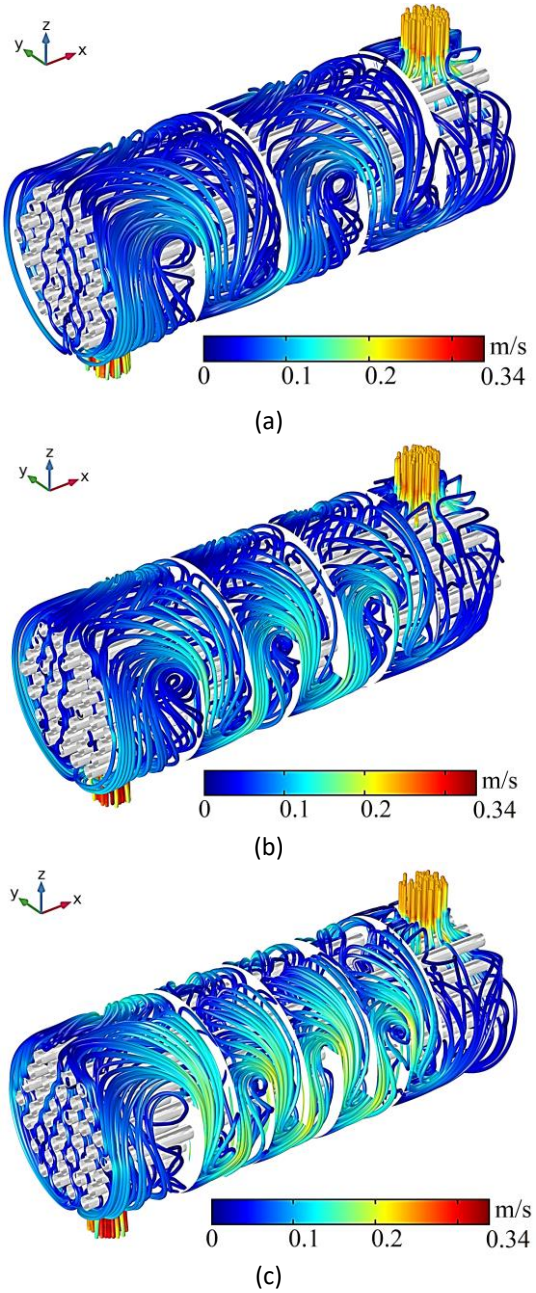

Fig. 4. Velocity streamlines distribution at 35% baffles cut and maximum mass flow rate (0.232 kg/s), (a) 4 baffles, (b) 6 baffles and (c) 8 baffles

Recirculation and dead zones had detrimental effects which retard heat transfer and help to provide a suitable condition for fouling. On the other hand, the cross-flow is observed to be well utilized as the number of baffles increases to 8 (Figure 4(c)) with a reduction in recirculation zones. This observation is consistent with the previous results of Ozden *et al*., [6], Mellal *et al*., [12] and Sadikin *et al*., [14].

3.3 Heat Transfer

As a reference case, the shell-side is simulated without baffles. This allows to compare the thermal performance of various baffles spacing and cut against the reference case without baffles. Figure 5 shows the distribution of Nusselt number and friction factor with nozzle-based Reynolds number for the reference case. Due to forced convection, Nusselt number increases when increasing the water inlet velocity. Meanwhile, the friction factor decreases with increasing Reynolds number due to a relatively increased flow resistance.

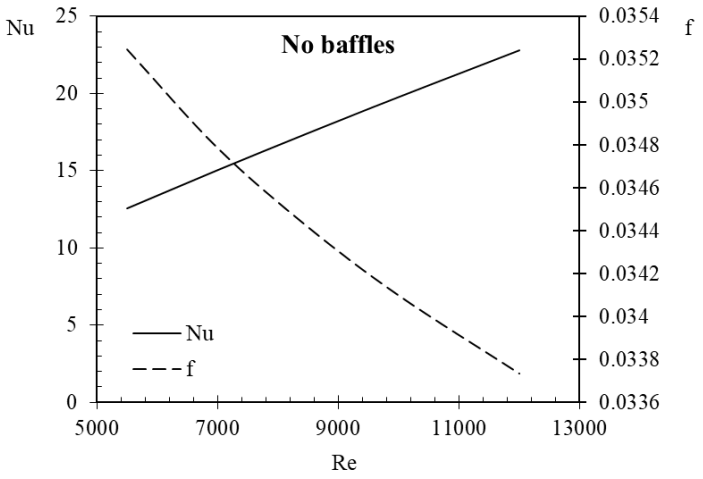

Fig. 5. Nusselt number and friction factor versus Reynolds number for the case of STHX without baffles

With the existence of baffles, an enhancement in the thermal shell-side performance is obtained for all investigated range of baffle spacings and cuts. Baffles not only used to support tubes but also to direct the flow in the shell-side for better mixing with tube-bundle. In general, increasing the number of baffles from 4 to 8 tends to augment the heat transfer coefficient for all baffle cuts. This can be demonstrated from the variation of the Nusselt number with Reynolds number for different baffles cut and spacing as shown in Figure 6.

In comparison with the reference case (without baffles), the maximum enhancement reached in Nusselt numbers at a maximum mass flow rate of 0.232 kg/s are 243%, 207%, and 152% with baffles cut, 25%, 35%, and 45%, respectively at maximum eight baffles. The case with 25% baffle cut had Nusselt number values 11% and 36% higher than that of 35% and 45% baffles cut, respectively, at the same number of baffles (8) and mass flow rate (0.232 kg/s). The smaller spacing between baffles augments heat transfer coefficient due to the intensified turbulence level and the local mixing.

This is clearly observed from streamlines temperature distribution for different baffles spacing and 35% baffles cut as shown in Figure 7. The zigzag flow pattern through a shorter bypass between baffles ensures more fluid mixing and better heat transfer rates. This can be verified from the increased calculated weighted average temperatures at the outlet of the nozzle varying from 319 K, 323 K to 326 K as the number of baffles increases from 4, 6 to 8, respectively. Contrary to Sadikin *et al*., [14] results, the current CFD results agree well with the results of Ozden *et al.,* [6] and Mellal *et al.,* [12] on that an increase in the number of baffles increases shell-side outlet temperature at the same mass flow rate.

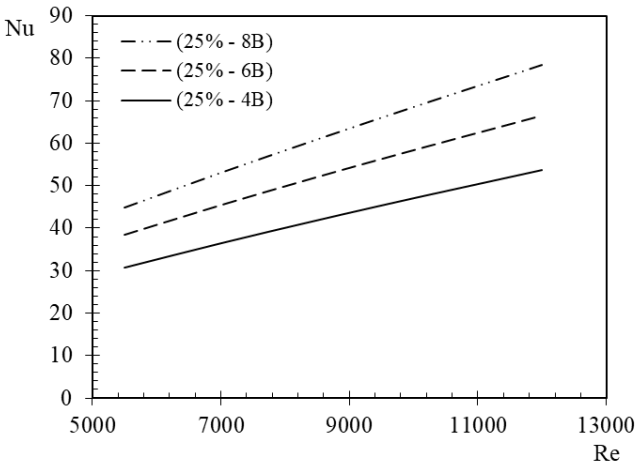

(a)

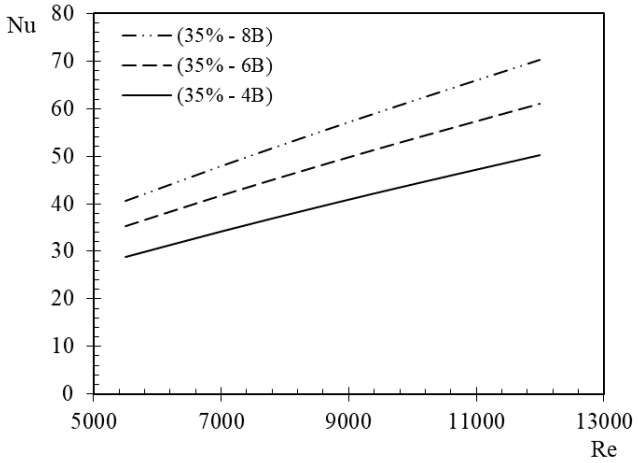

(b)

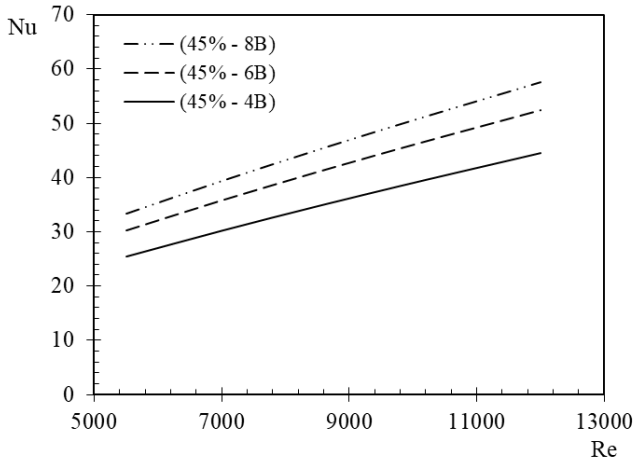

(c)

Fig. 6. Nusselt number versus Reynolds number for different baffles cut and spacing

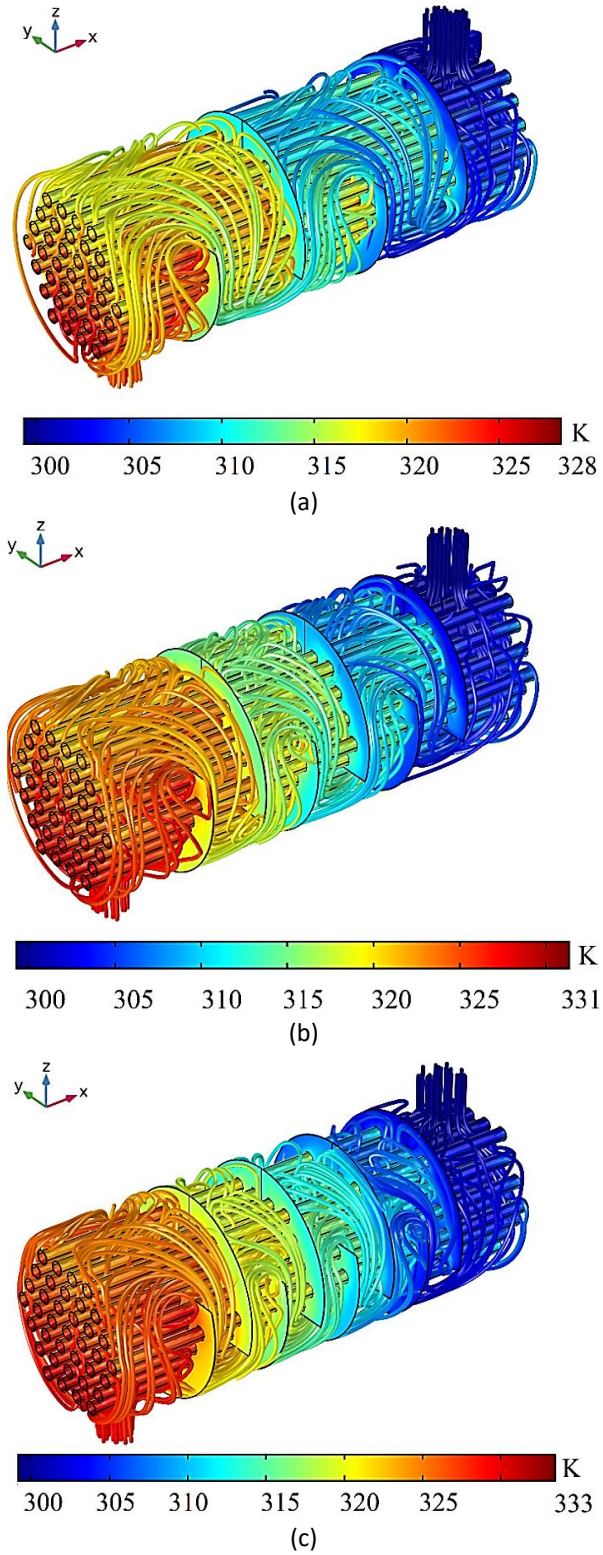

Fig. 7. Streamlines temperature distribution at 35% baffles cut and maximum flow rate (0.232 kg/s), (a) 4 baffles, (b) 6 baffles and (c) 8 baffles

3.4 Pressure Drop

The variation of friction factors with Reynolds number at different baffle spacing and baffle cut is illustrated in Figure 8. The friction factors are strongly influenced by the variation of baffle spacing

and baffle cut. In general, because of abrupt momentum change and pressure drop due to extra flow resistance, friction factors increase with reducing both baffles spacing and cut which agrees with the findings of Ozden *et al*., [6] and Mellal *et al*., [12].

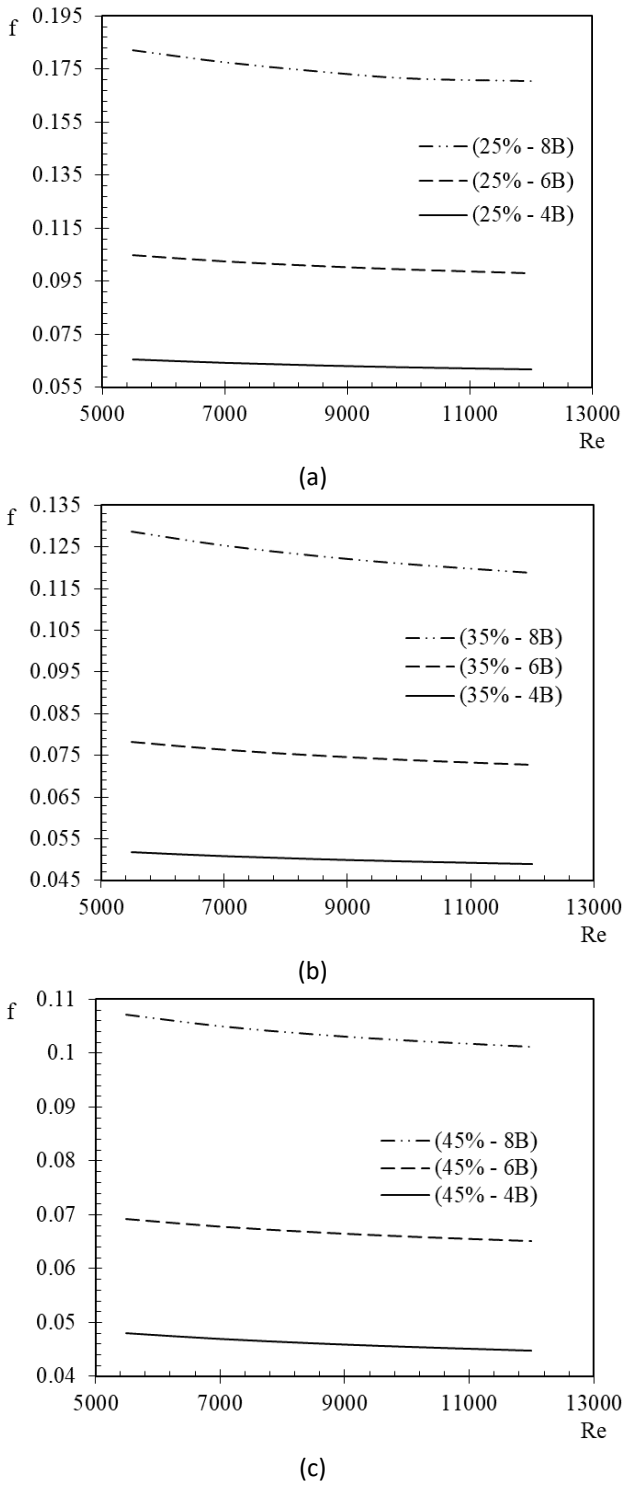

Fig. 8. Variation of friction factors with Reynolds number at different baffle spacing and baffle cut

Higher friction factors are observed for the case of 25% baffles cut and a maximum number of 8 baffles (shorter bypass or spacing) which had the best thermal characteristics among the other cases.

In comparison with the baseline case, the maximum difference recorded of friction factor to that obtained at 25% baffles cut is 417% at a minimum mass flow rate. The friction factor values are considerably reduced by increasing baffles cut from 25% to 45% at a fixed number of baffles. Therefore, another factor is required to judge the thermal performance of STHX based on a good compromise between heat transfer and pressure drop.

3.5 Thermal Performance Factor

To judge the hydro-thermal performance of the STHX, the definition of the thermal performance factor (η) was introduced to compare all investigated configurations. This factor is based on the constraint of equal pumping power. The variation of (η) versus Reynolds number is demonstrated in Figure 9. Nine geometrical configurations are realized: three cases of baffle spacing (100, 60 and 42.85 mm) corresponding respectively to the number of baffles: 4, 6 and 8 and three cases of baffle cut (25, 35 and 45%). All performance factors are observed to be more than 1.75, where the maximum value of 2.15 is achieved with the case of 6 baffles and 35% baffle cut at a minimum mass flow rate (Re = 5,500). This configuration is highly recommended to replace the current STHX for an efficient energy exchange.

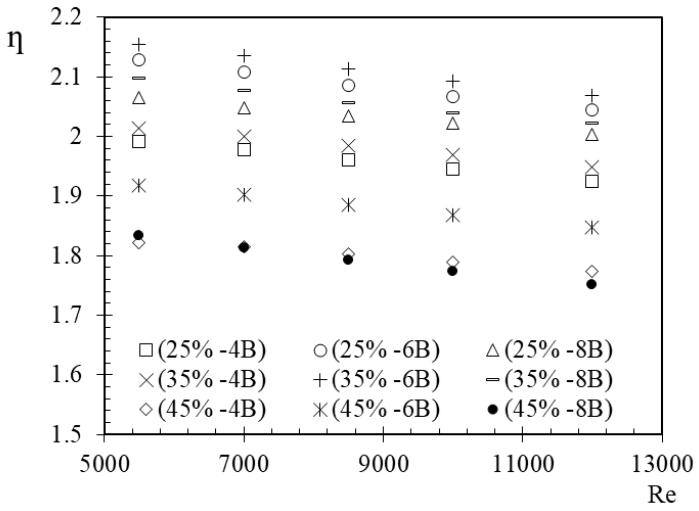

Fig. 9. Thermal performance factor vs. Reynolds number for all investigated configurations

4. Conclusions

Hydro-thermal characteristics in the shell-side of a shell-and-tube heat exchanger fitted with single segmental baffles were numerically analysed using 3D CFD simulations. Three geometrical configurations with different baffles spacing are realized, which are: 100, 60, and 42.85 mm. These values correspond respectively to the baffle numbers: 4, 6 and 8 baffles. The effects of the baffle cut (25%, 35%, and 45%) are also studied. The investigations are conducted with Reynolds number (based on inlet nozzle hydraulic diameter) ranging from 5,500 to 12, 000. The following conclusions are drawn and summarized

i. The STHX performance is affected by the change in baffle spacing where heat transfer coefficient and the pressure drop increase by reducing the baffles spacing or increasing the number of baffles.

ii. For efficient STHX design, the baffle cut is another parameter needs to be optimised. Reducing baffle cut results in an increase in both heat transfer and pressure drop. The case of lower spacing (8 baffles) and lower baffle cut (25%) had the highest heat transfer coefficient with a penalty of highest pressure drop.

iii. The best thermal performance factor of (η = 2.15) was obtained for the case of 6 baffles cut by 35% at Re = 5,500. This configuration provides a good compromise between heat transfer and pressure drop at equal pumping power constraint.

Turbulence and conjugate heat transfer modelling in CFD analysis of heat exchangers are more comprehensive and demanding in terms of accuracy, stability and computational time. Continuous meshing in such a complex 3D heat exchanger geometry consumes more memory which is limited to the available computational resources. For future work, adopting discontinuous meshing technique for conjugate heat transfer modelling can be promising as the number of mesh elements is considerably reduced and hence time-saving solution is reached.

References

[1] Lee, Y. K. "The use of nanofluids in domestic water heat exchanger." *Journal of Advanced Research in Applied Mechanics* 3, no. 1 (2014): 9-24.

[2] Holman, Jack P. *Heat transfer*. McGraw-hill, 2010.

[3] Towler, Gavin, and Ray Sinnott. *Chemical engineering design: principles, practice and economics of plant and process design*. Elsevier, 2012.

[4] Bhutta, Muhammad Mahmood Aslam, Nasir Hayat, Muhammad Hassan Bashir, Ahmer Rais Khan, Kanwar Naveed Ahmad, and Sarfaraz Khan. "CFD applications in various heat exchangers design: A review." *Applied Thermal Engineering* 32 (2012): 1-12.

[5] Nemati, Hossain, and Mohammad Moghimi. "Numerical study of flow over annular-finned tube heat exchangers by different turbulent models." *CFD Letters* 6, no. 3 (2014): 101-112.

[6] Ozden, Ender, and Ilker Tari. "Shell side CFD analysis of a small shell-and-tube heat exchanger." *Energy Conversion and Management* 51, no. 5 (2010): 1004-1014.

[7] Wen, Jian, Huizhu Yang, Simin Wang, Yulan Xue, and Xin Tong. "Experimental investigation on performance comparison for shell-and-tube heat exchangers with different baffles." *International Journal of Heat and Mass Transfer* 84 (2015): 990-997.

[8] Ambekar, Aniket Shrikant, R. Sivakumar, N. Anantharaman, and M. Vivekenandan. "CFD simulation study of shell and tube heat exchangers with different baffle segment configurations." *Applied Thermal Engineering* 108 (2016): 999-1007.

[9] El Maakoul, Anas, Azzedine Laknizi, Said Saadeddine, Mustapha El Metoui, Abdelkabir Zaite, Mohamed Meziane, and Abdelatif Ben Abdellah. "Numerical comparison of shell-side performance for shell and tube heat exchangers with trefoil-hole, helical and segmental baffles." *Applied Thermal Engineering* 109 (2016): 175-185.

[10] Bayram, Halil, and Gökhan Sevilgen. "Numerical investigation of the effect of variable baffle spacing on the thermal performance of a Shell and tube heat Exchanger." *Energies* 10, no. 8 (2017): 1156.

[11] Lei, Yonggang, Yazi Li, Shenglan Jing, Chongfang Song, Yongkang Lyu, and Fei Wang. "Design and performance analysis of the novel shell-and-tube heat exchangers with louver baffles." *Applied Thermal Engineering* 125 (2017): 870-879.

[12] Mellal, Mustapha, Redouane Benzeguir, Djamel Sahel, and Houari Ameur. "Hydro-thermal shell-side performance evaluation of a shell and tube heat exchanger under different baffle arrangement and orientation." *International Journal of Thermal Sciences* 121 (2017): 138-149.

[13] Wang, Xinting, Nianben Zheng, Zhichun Liu, and Wei Liu. "Numerical analysis and optimization study on shell-side performances of a shell and tube heat exchanger with staggered baffles." *International Journal of Heat and Mass Transfer* 124 (2018): 247-259.

[14] Sadikin, A., N. Y. Khian, Y. P. Hwey, H. Y. Al-Mahdi, I. Taib, A. N. Sadikin, S. Md Salleh, and S. S. Ayop. "Effect of Number of Baffles on Flow and Pressure Drop in a Shell Side of a Shell and Tube Heat Exchangers." *structure* 48, no. 2 (2018): 156-164.

[15] Amini, Reza, Mohsen Amini, Alireza Jafarinia, and Mehdi Kashfi. "Numerical investigation on effects of using segmented and helical tube fins on thermal performance and efficiency of a shell and tube heat exchanger." *Applied Thermal Engineering* 138 (2018): 750-760.

[16] Arani, Ali Akbar Abbasian, and Reza Moradi. "Shell and tube heat exchanger optimization using new baffle and tube configuration." *Applied Thermal Engineering* 157 (2019): 113736.
[17] Comsol multiphysics, CFD, heat transfer modules., Version 5.3 (2017).
[18] Lee, Ho Sung. *Thermal design: heat sinks, thermoelectrics, heat pipes, compact heat exchangers, and solar cells*. John Wiley & Sons, 2010.
[19] Kern, Donald Quentin. *Process heat transfer*. Tata McGraw-Hill Education, 1997.
[20] Bejan, Adrian, and Allan D. Kraus. *Heat transfer handbook*. Vol. 1. John Wiley & Sons, 2003.